Wide lag time distributions break a trade-off between reproduction and survival in bacteria

Stefany Moreno-Gámez[a,b,c,1], Daniel J. Kiviet[a,b], Clément Vulin[a,b,d], Susan Schlegel[a,b,e], Kim Schlegel[a,b], G. Sander van Doorn[c,2], and Martin Ackermann[a,b,2]

[a]Institute of Biogeochemistry and Pollutant Dynamics, Department of Environmental Systems Science, ETH Zurich, 8092 Zurich, Switzerland; [b]Department of Environmental Microbiology, Eawag, 8600 Dübendorf, Switzerland; [c]Groningen Institute for Evolutionary Life Sciences, University of Groningen, 9700 CC Groningen, The Netherlands; [d]Division of Infectious Diseases and Hospital Epidemiology, University Hospital Zurich, University of Zurich, 8091 Zurich, Switzerland; and [e]Department of Cell and Molecular Biology, Uppsala University, 75124 Uppsala, Sweden

Edited by Bruce R. Levin, Emory University, Atlanta, GA, and approved May 28, 2020 (received for review February 27, 2020)

Many microorganisms face a fundamental trade-off between reproduction and survival: Rapid growth boosts population size but makes microorganisms sensitive to external stressors. Here, we show that starved bacteria encountering new resources can break this trade-off by evolving phenotypic heterogeneity in lag time. We quantify the distribution of single-cell lag times of populations of starved *Escherichia coli* and show that population growth after starvation is primarily determined by the cells with shortest lag due to the exponential nature of bacterial population dynamics. As a consequence, cells with long lag times have no substantial effect on population growth resumption. However, we observe that these cells provide tolerance to stressors such as antibiotics. This allows an isogenic population to break the trade-off between reproduction and survival. We support this argument with an evolutionary model which shows that bacteria evolve wide lag time distributions when both rapid growth resumption and survival under stressful conditions are under selection. Our results can explain the prevalence of antibiotic tolerance by lag and demonstrate that the benefits of phenotypic heterogeneity in fluctuating environments are particularly high when minorities with extreme phenotypes dominate population dynamics.

life history trade-offs | phenotypic minorities | antibiotic tolerance | starvation | single-cell dynamics

In nature bacteria live in highly dynamic environments where they rarely experience a constant nutrient supply. Instead, conditions often alternate between periods of starvation and resource abundance (1–3). When encountering new resources, starved bacterial populations do not resume growth immediately but rather show a delay at the population level known as lag time. This delay can have important consequences for the long-term population dynamics because of the fundamental trade-off between reproduction and survival that underlies transitions between growing and nongrowing states: Although there is a direct benefit to rapid growth resumption, nongrowing cells are less susceptible to external stressors than actively dividing cells.

Slowly or nondividing bacterial cells are particularly relevant in the context of bacterial infections because they can survive antibiotic exposure without being genetically resistant to antibiotics (4, 5). Such cells can arise by stochastic phenotype switching from cells in stationary or exponential phase and are then known as persisters (4, 6–9). While various empirical and theoretical studies have investigated the emergence and dynamics of subpopulations of persisters (10, 11), much less is known about how delayed growth resumption from starvation can lead to increased survival to antibiotics [a phenomenon known as tolerance by lag (12)]. In particular, both the extent of variation in lag time at the single-cell level and its consequences for population growth and survival are unresolved.

Here, we quantify phenotypic variation in lag time in clonal populations of bacteria and combine these observations with selection experiments and mathematical modeling to investigate the evolution of lag time distributions. We start by quantifying lag time distributions by direct observation of single cells coming out of starvation; the resulting data reveal substantial variation in lag between individual cells, which increases with the duration of starvation and depends on the nature of the resource encountered upon growth resumption. Next, we investigate the evolution of lag time distributions by studying the consequences of lag time variation on population growth and survival. We show experimentally that bacteria evolve narrow lag time distributions upon repeated passage through feast-and-famine cycles when selection consistently favors rapid growth. However, for a fluctuating regime of selection on both growth and survival, modeling predictions indicate that bacteria can resolve the resulting trade-off between these two fitness components by evolving phenotypic heterogeneity in lag. We show that this strategy is particularly effective because cells in the opposite extremes of the lag time distribution have a disproportionate effect on growth and survival at the population level: While growth is dominated by the cells with shortest lag times, tolerance to antibiotic stress is provided by the cells with longest lag times.

Significance

The biology of many microorganisms has been adapted to a feast-and-famine lifestyle. Thus, understanding population dynamics during transitions from starvation to resource abundance is important for fundamental and applied reasons. Here, we study starved populations of bacteria encountering new resources and ask how the behavior of single cells gives rise to emergent population-level traits. We find that growth and survival of populations are dominated by phenotypic minorities: small subpopulations with extreme lag times. As a consequence, starved populations of bacteria can break a fundamental life history trade-off between growth and survival by evolving phenotypic variation in lag time. By showing why bacteria can sustain subpopulations with long lag times our findings can explain the prevalence of antibiotic tolerance by lag.

Author contributions: S.M.-G., D.J.K., G.S.v.D., and M.A. designed research; S.M.-G., D.J.K., C.V., S.S., and K.S. performed research; S.M.-G. and G.S.v.D. contributed new reagents/analytic tools; S.M.-G. analyzed the data with feedback from G.S.v.D. and M.A.; and S.M.-G., G.S.v.D. and M.A. wrote the manuscript with feedback from the other authors.

The authors declare no competing interest.

This article is a PNAS Direct Submission.

Published under the PNAS license.

Data deposition: Sequencing reads are publicly available on the European Nucleotide Archive (ENA) database under accession number PRJEB38320. The code for the simulations is available at DataverseNL (https://hdl.handle.net/10411/TBLEFB).

[1]To whom correspondence may be addressed. Email: s.moreno.gamez@rug.nl.

[2]G.S.v.D. and M.A. contributed equally to this work.

This article contains supporting information online at https://www.pnas.org/lookup/suppl/doi:10.1073/pnas.2003331117/-/DCSupplemental.

First published July 15, 2020.

Downloaded at Palestinian Territory, occupied on December 31, 2021

www.manaraa.com

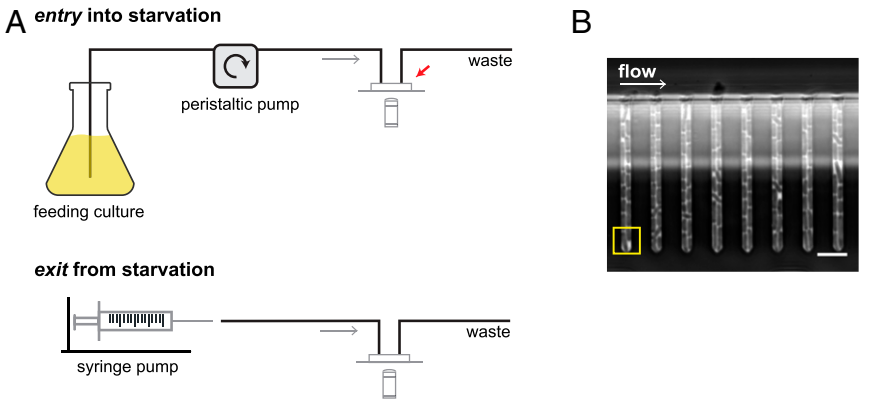

Fig. 1. Quantifying lag time distributions after prolonged starvation. (*A*) Microfluidic setup to quantify lag times at the single-cell level. (*Top*) Bacteria are loaded into a microfluidic device (indicated by the red arrow) and monitored using time-lapse microscopy. The device is connected to a batch culture inoculated at low density. In this way, cells in the microfluidic device experience conditions similar to the bacteria in the batch culture: They first grow exponentially until resources are depleted and then become starved. (*Bottom*) Starvation stops when the device is disconnected from the batch culture and switched to fresh media. (*B*) We use a microfluidic device with a "mother machine" design, which enables following single cells through their entry, stay, and exit from the stationary phase. For all of the analyses presented in this paper, only the behavior of the cells at the bottom of a growth channel was quantified (yellow box). (Scale bar, 5 μm.)

Results

We developed a microfluidics setup to measure the lag time distributions of clonal *Escherichia coli* populations resuming growth after carbon starvation (Fig. 1). Bacteria were loaded in a microfluidic device and continuously monitored using time-lapse microscopy. Cells were starved for carbon by connecting the device to a batch culture growing from exponential to stationary phase in M9 minimal media with glucose, similar to a previously developed approach (7). From the time the batch culture was inoculated, bacteria were followed in the microfluidic device for different durations of starvation (*Methods*). After this time, we supplied the starved bacteria with fresh media and quantified their lag time at the single-cell level. We studied growth resumption in M9 minimal media with two different carbon sources (either glucose or lactose) since in nature bacteria might commonly resume growth in a different carbon source than the one they encountered before starvation. When switching between alternative carbon sources, actively dividing cell populations are known to exhibit diauxic growth with a phase of growth retardation at the moment when cells switch from utilizing one carbon source to the other. In combination with prolonged starvation such diauxie can lead to long population-level lag times (*SI Appendix*, Fig. S1) due to the time and resources that cells need to invest into expressing proteins to metabolize a new carbon source (13). In order to investigate this effect, we compared growth resumption with and without a change in the available carbon source. We used lactose as the alternative resource because it exhibits a long population-level lag while yielding a growth rate similar to that of glucose (*SI Appendix*, Fig. S1).

The lag time quantification at the single-cell level was consistent with the population-level measurements and showed that bacteria take, on average, longer to resume growth in lactose than in glucose after prolonged starvation (Fig. 2*A*). More importantly, the observed distribution of lag times revealed that growth resumption is very heterogeneous among genetically identical cells, especially when cells experience a diauxic shift from glucose to lactose upon growth resumption. To further disentangle the role of starvation and diauxie on lag, we measured the lag time distributions of bacteria resuming growth in lactose both after short starvation and directly from exponential growth in glucose. Interestingly, we found that starvation and diauxie have a synergistic effect on lag time (Fig. 2*B*). This synergy may originate from a combination of the stochasticity in the dissociation of the *lac* repressor from the *lac* operon (14) and the low energetic state of cells coming out of starvation, which can result in many repressor dissociation events not ending in successful protein production. Nonetheless, such synergy is not merely a consequence of protein expression since we find that even if bacteria are induced to express the *lac* operon before starvation, growth resumption in lactose is still slower than in glucose (*SI Appendix*, Fig. S4). We hypothesize that in addition to the expression of the *lac* operon, the activity of the *lac* permease can be particularly costly for cells coming out of starvation because this protein operates using the proton motive force (PMF) of the cell (15), which gets depleted

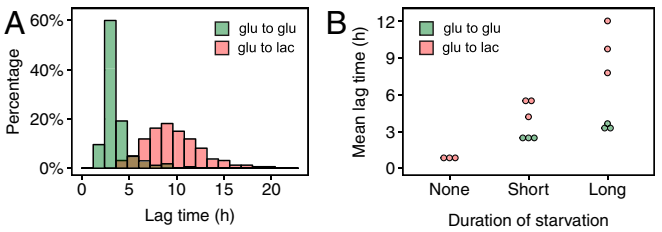

Fig. 2. The mean and variance of the lag time distribution depend on the nature of the resource switch. (*A*) Lag time distributions of *E. coli* MG1655 resuming growth in M9 media with either glucose (green) or lactose (red) after prolonged starvation in M9 media with glucose (40 h growth cycle where cells spend ~32 h starved). Histogram data come from one replicate for each condition. Distributions for two additional replicates for each condition are in *SI Appendix*, Fig. S2. Lag time is quantified as time to first division once fresh media is supplied. Lactose and glucose concentrations are 1.11 mM. (*B*) Mean lag time as a function of the duration of starvation and the resource switch. "Long" starvation corresponds to the data presented in *A*, where a growth cycle lasts 40 h. "Short" starvation corresponds to growth cycles of 16 to 18 h (~8 h of starvation). "None" corresponds to a diauxic shift where cells are switched to lactose while growing in exponential phase in glucose. Lag time for the diauxic shift is calculated as the difference between the interdivision time before and after the switch to lactose (see *Methods* and *SI Appendix*, Fig. S3 for details). The increase in both the mean and the variance of the lag time distribution with the duration of starvation is higher when bacteria resume growth in lactose than when they resume growth in glucose. These interactions are significant, as shown by two mixed effects models ($F = 79.8$ and $F = 62.5$ for the mean and the variance, respectively, with $P < 0.005$ for both cases). Three independent replicates are shown for every condition. Each replicate corresponds to data for at least 130 cells.

Downloaded at Palestinian Territory, occupied on December 31, 2021
www.manaraa.com

during starvation. This could explain the consistent population-level difference in lag time that we observe for sugars imported by PMF or ATP-dependent transporters versus sugars imported using phosphotransferase systems (like glucose) (*SI Appendix*, Fig. S1) since the latter rely on phosphoenolpyruvate, a metabolic intermediate that transiently increases upon carbon starvation in *E. coli* unlike the PMF or ATP (16).

Importantly, such strong variation in lag time that we find for switches to lactose can have major consequences for population growth: Given that after prolonged starvation early and late responders differ in lag time by more than 10 hours (corresponding to approximately 10 times the doubling time in exponential phase in lactose), the fastest cells to resume growth can leave on the order of 1,000 times (2^{10}) more offspring to the newly formed population than their genetically identical sister cells that resumed growth 10 h later.

Motivated by this observation, we asked whether bacteria could attain a narrow lag time distribution where all cells resume division as soon as resources become available since this would be the best possible strategy for rapid growth after starvation for an isogenic population. We did this by evolving *E. coli* in a regime that selects for rapid growth in lactose after prolonged starvation, using a serial dilution setup that mimics the conditions for our microfluidic measurements: Bacteria were inoculated in M9 minimal media with glucose, and after 40 h, the starved cultures were diluted in M9 minimal media with lactose. Bacteria remained in this fresh media for only 8 h, after which they were transferred back into M9 with glucose, restarting a selection cycle (*SI Appendix*, Fig. S5). We evolved six independent populations under this regime for ∼600 generations using as the ancestor *E. coli* MG1655.

The evolved populations rapidly improved their performance relative to the ancestor (*SI Appendix*, Fig. S5). This is consistent with the dynamics of a long-term evolution experiment with *E. coli* where lag time was one of the traits with the steepest selection response during the first 2,000 generations of a feast-and-famine regime (17). Moreover, we found that the lag time distribution became much narrower in all populations (Fig. 3), which indicates that *E. coli* can move toward an optimal distribution for fast growth resumption where all cells start dividing very quickly after resources become available. Sequencing revealed that all populations accumulated mutations in the *lac* operon repressor, LacI, leading to constitutive derepression of the *lac* operon (*SI Appendix*, Table S1) (18). This observation further confirms that one of the main bottlenecks for growth resumption in lactose after prolonged starvation in glucose is the expression of the *lac* operon. In addition, most of the populations accumulated mutations in a family of proteins linked to nitrogen starvation, YeaH and YeaG (19), in the *rph-pyrE* operon (20) and in different subunits of the RNA polymerase (*SI Appendix*, Table S1).

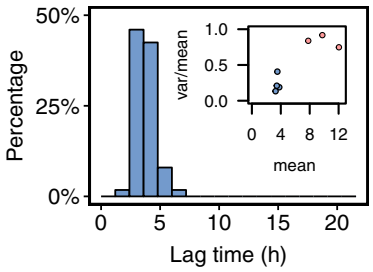

Fig. 3. Phenotypic heterogeneity in lag time can be reduced upon prolonged selection for rapid growth resumption after starvation. Distribution of lag times of a single clone isolated from an evolved population resuming growth in M9 media with lactose after prolonged starvation in M9 media with glucose. The concentration of both sugars is 1.11 mM as in Fig. 2. The clone was isolated from one of six replicate populations after ∼600 generations of selection for reduced lag time in lactose after starvation. The *Inset* shows summary statistics (mean and variance-to-mean ratio) for three replicate measurements of the ancestor (red dots) and four clones isolated from independent populations at the end of the evolution experiment, including the one shown in the histogram (blue dots). The clone shown in the main figure is 1Gc. See *SI Appendix*, Fig. S6 and Table S1 for the distributions of the remaining clones and for the genetic information for all clones.

Although this evolution experiment establishes that long lag times are costly and that bacteria can rapidly change their lag time distributions in response to selection for fast growth (Fig. 3 and *SI Appendix*, Figs. S5 and S6), short lag times are not necessarily beneficial under all conditions. In particular, in the presence of antibiotics, delaying the resumption of growth after the appearance of new resources can be vital to survive a window of antibiotic exposure. Support for this idea comes from experiments that show that bacteria evolve longer lag times when they are exposed to a pulse of antibiotics at the time that new nutrients appear (12), conditions that favor the survival of cells that are tolerant by lag.

To further study the trade-off between growth and survival, we analyze how the lag time distribution determines both of these fitness components in a clonal population. We start by focusing on population growth and study how population-level performance is determined by the lag time distribution. Importantly, a basic feature of the growth dynamics is that there is a nonlinear relationship between the lag time of a cell and fitness at the individual level, defined here as the number of progeny contributed by a cell to the growing population in a specific time period: Due to the nature of bacterial growth, this number will decrease exponentially with a cell's lag time. To illustrate this, consider a single cell with lag time τ. Assuming that this cell starts dividing exponentially at rate r once it exits lag, the number of descendants that it will have at time t is given by $N(t) = 2^{r(t-\tau)}$ for $t > \tau$. Accordingly, the number of offspring of a lagging cell is reduced by a factor $2^{r\tau}$, relative to a cell that resumes growth immediately after resources appear.

To study how this nonlinearity affects population growth resumption when lag time distributions are heterogeneous, we developed a simple mathematical model. We assume that every cell in a population samples a lag time from a distribution determined by the population's genotype. When resources become available, cells wait for that amount of time and then resume growth at their maximum growth rate. In addition, we assume that once bacteria resume growth, they remain in exponential phase. We model lag time distributions as gamma distributions, which are a family of distributions commonly used to describe waiting times. Using these assumptions, we derive an equation for the size at time t of a clonal population that is initiated from N_0 cells with heterogeneous lag times that resume growth after starvation,

$$N(t) = \frac{N_0 2^{rt}}{[1 + \upsilon r \log(2)]^{u/\upsilon}}. \quad [1]$$

Here, r is the doubling rate, and u and v are the parameters determining the shape of the lag time distribution of the population with $E[\tau] = u$ and $Var[\tau] = uv$ (*SI Appendix*). The numerator of Eq. **1** corresponds to classical exponential growth, while the denominator can be interpreted as the cost for the population of not resuming division as soon as resources appear. Naturally, this cost increases with the mean lag time u. Also, it increases with r, reflecting that genotypes that are fast growers pay a higher cost for not resuming growth as soon as starvation ends. Importantly, this cost decreases if the variance in lag time increases or, more precisely, if the variance-to-mean ratio of the lag time distribution v increases. Thus, the fitness of a genotype will be strongly influenced by the shape of its lag time distribution and

Downloaded at Palestinian Territory, occupied on December 31, 2021

www.manaraa.com

not only by its mean. In fact, a cell whose lag time corresponds to the arithmetic mean of the population contributes to the growing population less than the average number of progeny because the dynamics of growth resumption satisfies Jensen's inequality (21) (*SI Appendix*). We illustrate this concept by simulating the dynamics of growth resumption of two populations with different lag time distributions (Fig. 4*A*). Although the blue population has shorter mean lag time than the red population, the latter has a better overall performance when resuming growth out of starvation.

The inherent nonlinearity of the process of exponential growth explains why the shape of the lag time distribution has such a strong effect on fitness: When new resources appear, overall growth resumption is dominated by the cells with shortest lag. Therefore, as previous models of lag time have shown (22, 23), the performance of a population will be mainly determined by the position of the left tail of its lag time distribution, which is where the earliest responders are located. We quantified this effect by plotting the cumulative offspring distribution of our simulated populations. In the population with high variance in lag, the 5% of individuals that resume growth in the first 5 h produce more than 70% of the descendant population, whereas in the population with low variance in lag, offspring sizes are much more evenly distributed (Fig. 4*B*). Thus, although the lag times of the majority of individuals in the heterogeneous population are equal to or higher than those of the homogeneous population, growth resumption in the former is dominated by the small fraction that resumes growth very early (before the bulk of the homogenous population). Importantly, this shows that the presence of some individuals with long lag times does not incur a substantial cost for clonal populations.

We now switch our attention to the other component of the trade-off and study how lag time distributions affect population survival. It is known that actively dividing cells are more susceptible than nongrowing cells to external stressors and particularly to antibiotics (6, 12, 24). Using our microfluidics setup, we asked whether a population of bacteria with a heterogeneous lag time distribution would benefit from having some cells with long lag times as these cells would remain protected from antibiotic stress for longer. To do so, bacteria were starved in glucose and switched to M9 with lactose as before (Fig. 1). Then, an antibiotic pulse was applied 8.6 h after the switch to fresh media, a time window that was chosen to ensure that when the pulse is applied some cells have already resumed growth while others remain in lag phase. The pulse lasted for 80 min and consisted of the same growth media with 100 μg mL^{-1} of ampicillin. We followed bacteria for 20 h after the pulse was applied and kept track of every division and lysis event from the time when lactose was provided. We found that cells that had not divided before the pulse were significantly more likely to survive antibiotic exposure than cells that had already divided (Fig. 5). In addition, we observed that after removal of the antibiotic, the lag time distribution appears unaffected (*SI Appendix*, Fig. S7). The latter suggests that antibiotic exposure has a minor effect on the process of growth resumption that underlies the lag time distribution.

Importantly, we repeated this experiment for the less heterogeneous switches studied before (Fig. 2*B*) and found that tolerance, measured as the fraction of cells that survives the pulse, decreases in the absence of either diauxie or starvation (*SI Appendix*, Fig. S8). This demonstrates that tolerance by lag is a trait that is highly contingent on the nature of environmental fluctuations unlike other less context-dependent traits like antibiotic resistance. We also applied a pulse of antibiotics to the evolved strains and found that as a consequence of selection for rapid growth resumption, these strains became less tolerant to antibiotics upon the same glucose to lactose shift (*SI Appendix*, Fig. S9). This shows how mutations targeting bacterial metabolism can affect antibiotic tolerance and further emphasizes the trade-off between growth and survival underlying feast-and-famine regimes.

We then asked whether there are environmental regimes that would select for high variance in lag time. To explore this question, we extended our previous mathematical model to study the evolution of lag time distributions. As before, we assumed that an individual cell samples its lag time from a gamma distribution. The parameters of this distribution are determined by two evolving traits: the mean lag time u and the variance-to-mean ratio v. Using stochastic simulations, we first studied how lag time distributions evolve when there is only selection for rapid growth resumption. We assume that both u and v can mutate upon cell division with probability μ and that mutation is stepwise so the mutated trait goes up or down by a fixed step size δ. When new resources appear, bacteria sample a lag time and start dividing until the population reaches a set carrying capacity. Then, a small fraction of the final population is sampled at random to start a new growth cycle.

We find, as expected, that under selection for rapid growth resumption the mean lag time goes to zero (Fig. 6 *A* and *B*). As the mean lag time decreases, also the shape of the distribution responds to selection; in fact, model populations evolve toward the optimal homogeneous distribution by increasing the variance-to-mean ratio of the lag time distribution. Note that as v becomes higher, both extremes of the lag time distribution shift,

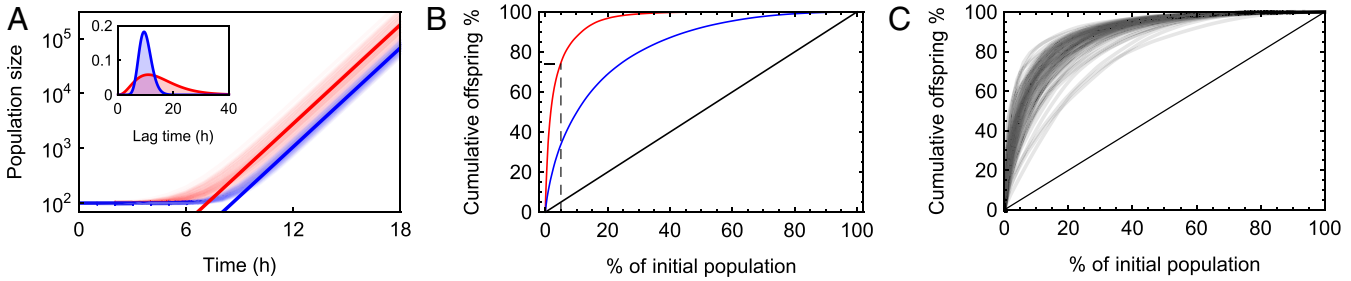

Fig. 4. Cells with the shortest lag times dominate population growth. (*A*) Growth curves of two populations with different lag time distributions (*Inset*) resuming growth after starvation. Light colors show 100 replicate stochastic growth trajectories simulated for each of the populations. Solid lines show the analytical predictions given by Eq. **1**. The mean lag time of the blue population is 10 h, and the mean lag time of the red population is 15 h. Despite having a higher mean lag time, the red population resumes growth faster than the blue population. Other parameters are $v_{blue} = 0.5$, $v_{red} = 4$, $N_0 = 100$, $r = 1\ h^{-1}$. (*B*) Simulated cumulative offspring distributions of the two populations shown in *A*. The $x = y$ line represents the scenario where every cell leaves exactly the same number of descendants once the population resumes growth after starvation. Both populations deviate from the neutral expectation, although the deviation is stronger for the red population. In this population, more than 70% of the offspring after starvation come from only 5% of the initial population (dashed lines). (*C*) Simulated cumulative offspring distributions of 100 populations with the lag time distribution measured for starved *E. coli* resuming growth in lactose (Fig. 2*A*). We assume that resources appearing after starvation are limited to simulate a more realistic scenario for bacteria in nature (*SI Appendix*). Cells with short lag rapidly resume growth and deplete resources. As a result, 10% of the initial population leaves on average more than 60% of the descendants. Parameters are $N_0 = 100$, K = 10,000, $r = 1\ h^{-1}$, where K is the carrying capacity.

Downloaded at Palestinian Territory, occupied on December 31, 2021
www.manaraa.com

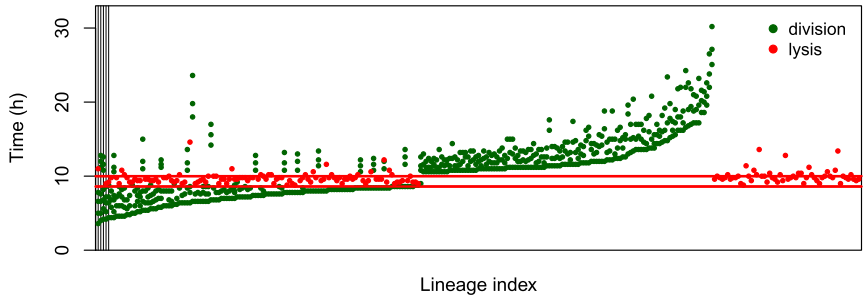

Fig. 5. Cells with long lag time are protected from antibiotics. Division and lysis events of an *E. coli* population exposed to an antibiotic pulse after resuming growth in lactose from starvation. Apart from the antibiotic pulse, experimental conditions are the same as in the glucose to lactose switch presented in Fig. 2*A*. During the pulse the M9 media with lactose was supplemented with 100 μg mL^{-1} of ampicillin. All dots on the same vertical line correspond to a single cell lineage, and lineages are sorted on the *x* axis by lag time. To illustrate this, vertical lines are shown for the first five cell lineages. The antibiotic pulse (red lines) was applied from 8.6 to 10 h after the switch to lactose (done at $t = 0$ h). We recorded every division event before and during the pulse. We assumed that if a cell had divided three times after the pulse, the cell survived antibiotic exposure, and we stopped recording division events. Cells that had not divided before the pulse had a significantly higher chance of surviving antibiotic exposure than cells that had divided before ($n = 291$; $\chi^2 = 80.85$; $P < 10^{-10}$). Note that some cells lyse without ever dividing (rightmost cells with only a red dot).

so there are not only more cells with shorter lag but also more cells with very long lags. This further illustrates that the fitness cost of having cells with long lag can be easily compensated by the presence of cells with shorter lag. Importantly, the extent to which selection for rapid growth resumption will lead to an increase of the variance-to-mean ratio of the lag time distribution depends on how tight the relationship between the mean and the variance is (*SI Appendix*, *Supplementary Discussion*). In particular, we assumed here that the variance can change independently from the mean, which favors increasing the variance-to-mean ratio as a strategy to reduce population lag. However, for an alternative parametrization of the gamma distribution, where the mean and the variance are more tightly coupled, the model predicts that the variance of the distribution decreases under sole selection for rapid growth resumption (*SI Appendix*, Fig. S10). This outcome reflects the results of our evolution experiment (Fig. 3), indicating that for the switches under selection in this experiment, the mean and the variance of the lag time distribution can be tightly linked due to the molecular mechanisms underlying lag in the experimental strain (*SI Appendix*, *Supplementary Discussion*).

We next studied the evolution of lag time distributions under selection for growth and survival. We assume that bacteria encounter an antibiotic pulse during a growth cycle with probability p. The pulse occurs at a fixed time T_a after new resources have been provided. Based on our experimental observations, we make two assumptions. First, we assume that cells that were already dividing before the pulse die at a much higher rate than cells that had not divided yet (Fig. 5). Second, we assume that the lag time of cells that had not divided before the pulse and survive it remains unchanged after the pulse (*SI Appendix*, Fig. S7). For extreme values of p, we find that selection is dominated by either growth or survival (Fig. 6*C*): When p is low, the major selective pressure is for rapid growth resumption. This corresponds to the scenario analyzed in Fig. 6*A*, where fitness increases with lower mean lag time and higher variance-to-mean ratio and its maximum if all cells resume growth right after starvation ends. By contrast, when p is high, bacteria evolve a homogeneous lag time distribution where all cells resume growth at time T_a, i.e., right after the antibiotic pulse. The reproduction–survival trade-off is more pervasive at intermediate probabilities of encountering the antibiotic pulse; under these conditions, neither immediate growth resumption on the new resource nor a long lag time for all cells in the population is favored by selection. Instead, for these conditions we find that bacteria evolve wide lag time distributions with intermediate mean (Fig. 6*C*). Finally, note that even if bacteria always encounter an antibiotic pulse ($p = 1$), a growth–survival trade-off can occur if the time of appearance of the pulse is unpredictable. In this scenario, we also find that wide lag time distributions are advantageous as a way to break such a trade-off (*SI Appendix*, *Supplementary Discussion* and Fig. S11).

Discussion

Bacteria in nature are often challenged to rapidly resume growth after prolonged periods of starvation. Here we developed a method to quantify lag times at the single-cell level and showed that populations of starved bacteria exhibit strong phenotypic heterogeneity in lag, especially when resuming growth in carbon sources that they did not metabolize before entering starvation. By combining our single-cell measurements with mathematical modeling, we further showed that this variation can allow bacterial populations to solve a fundamental life history trade-off between reproduction and survival and as a result sustain cells with long lag times that tolerate antibiotics. Moreover, for selection regimes where this trade-off is weak and either reproduction or survival dominates, our model captures the outcome of two separate evolution experiments (Fig. 6*C*). First, it predicts that a reproduction-dominated regime would select for bacteria with shorter lag times that become less tolerant to antibiotics, which was observed in the evolutionary experiment presented in this paper (Fig. 3 and *SI Appendix*, Fig. S9). Second, it predicts that a survival-dominated regime would select for bacteria with long lag times that resume growth after antibiotic exposure, as reported by Fridman et al. (12).

We focus here on survival after growth resumption, but bacteria can potentially solve other trade-offs inherent in their prevalent feast-and-famine lifestyle by diversifying phenotypically. For instance, one of the selective conditions that has shaped the growth and resource utilization strategies of many bacterial species originates from the decision on how to prepare for starvation (25): While inactivating growth machinery (e.g., dimerizing ribosomes) and up-regulating stress response genes can increase survival during starvation (1, 2, 26, 27), this strategy might delay growth resumption when resources appear. In fact, it has been shown that bacteria selected for increased survival during prolonged starvation become less competitive at growing in fresh media (28). Ultimately, the optimal amount of preparation for starvation will depend on the duration of this period, which might be often unpredictable for bacteria. Besides the duration of starvation, another variable that bacteria might often not be able to anticipate is the carbon source that they will encounter upon growth resumption. Metabolic trade-offs are known to be prevalent in microbes, and as a result, growth resumption in

Downloaded at Palestinian Territory, occupied on December 31, 2021

www.manaraa.com

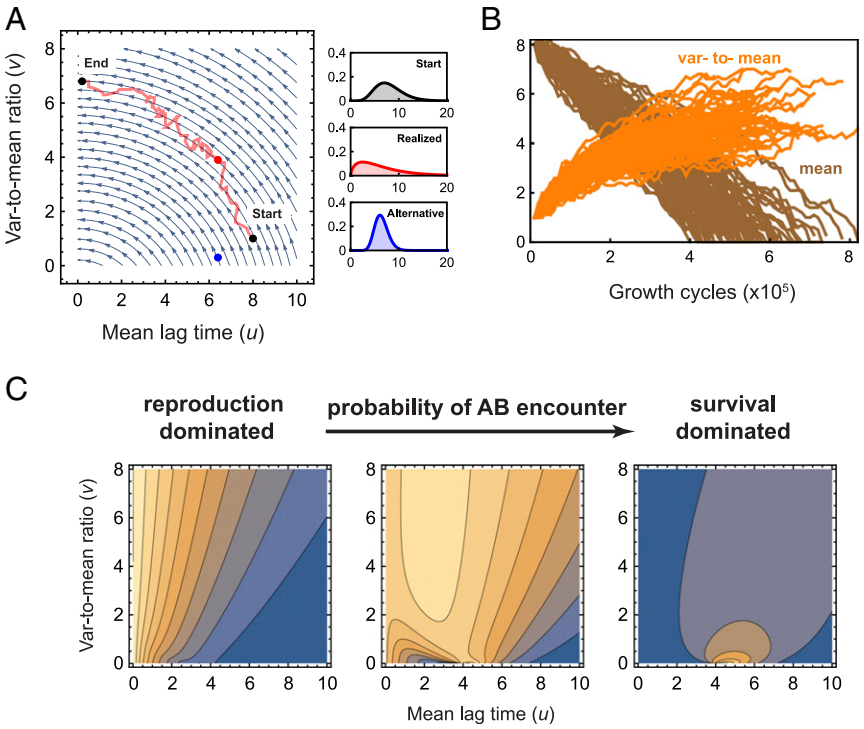

Fig. 6. Evolutionary dynamics of lag time distributions. (*A*, *Left*) Selection gradient calculated from Eq. **1** illustrating the directions of fitness increase when bacteria are selected for only rapid growth resumption. A trajectory of one representative evolutionary simulation is plotted on top of the selection gradient. As the mean lag time evolves to zero, the variance-to-mean ratio increases. These results are for a parameterization of the model where the mean and the variance-to-mean ratio of the lag time distribution can evolve as independent traits (see *SI Appendix*, Fig. S10 and *Supplementary Discussion* for results for an alternative parameterization). (*A*, *Right*) Lag time distributions of the initial population (black), an evolutionary intermediate population (red), and a hypothetical evolutionary intermediate where the lag time distribution would become narrower before shifting toward zero (blue). Despite lowering the mean lag time, such a hypothetical intermediate is not realized because the variance-to-mean ratio is under selection to increase. *B* highlights the generality of the pattern observed in *A* by showing evolutionary time series plots of mean and variance-to-mean ratio collected from 100 replicate simulations. Parameters are $N_0 = 100$, K = 500, $r = 1\ h^{-1}$, $\mu = 10^{-4}$, $\delta = 0.1$. (*C*) Fitness landscapes when there is simultaneous selection for reproduction and survival for varying probabilities of encounter p of an antibiotic pulse occurring at a fixed time T_a after the end of starvation. Fitness increases from blue to yellow. For all panels $T_a = 4$ h, $s_d = 0.001$, and $s_i = 0.7$, where s_d and s_i are the probabilities of surviving the antibiotic pulse for a cell that was dividing before the pulse and for a cell that was not dividing, respectively. (*Left*) When $p = 0.1$, selection is dominated by reproduction. Thus, the dynamics in this scenario is the same as in *A* and *B*, where the highest fitness is attained when the mean lag time is zero. (*Right*) When $p = 0.9$, selection is dominated by survival to the antibiotic pulse, so the highest fitness is attained if all cells resume growth right after the pulse. (*Middle*) When $p = 0.5$, bacteria maximize fitness by evolving distributions with intermediate mean and large variances. An alternative parameterization of the gamma distribution where the mean and lag time are more tightly linked also predicts the evolution of wide lag time distributions for intermediate values of p (*SI Appendix*, *Supplementary Discussion* and Fig. S10).

one carbon source might come at the cost of delayed growth resumption in other carbon sources (29–31). In both scenarios, variation in the duration of starvation (32, 33) or fluctuations in the type of new resources (31, 34) can lead to strong trade-offs that might be mitigated by phenotypic diversification resulting in lag time heterogeneity.

We have shown that phenotypic minorities on opposite sides of the lag time distribution can dominate population dynamics upon growth resumption. An important consequence of this finding is that populations of bacteria in nature, which often alternate between feast and famine regimes, might frequently go through tight bottlenecks where individuals with extreme lag times produce most of the offspring after starvation. We determined the extent of this effect for the quantified distribution of lag times in lactose after prolonged starvation and found high levels of reproductive skew (Fig. 4*C*). Moreover, we expect that this effect is of a similar magnitude for transitions to various other carbon sources given the long lags observed at the population level (*SI Appendix*, Fig. S1). Skewed offspring distributions in bacteria were recently documented in other contexts (35) and can strongly affect bacterial population dynamics because they lower the effective population size, amplifying the effect of genetic drift (36).

In addition to continuously tuning their phenotypes, isogenic populations of microbes can adapt to their ever-changing environments by diversifying phenotypically. In this way, a fraction of the population is always prepared for future environmental regimes at the cost of performing poorly in the current conditions. For example, microbes might use this strategy to survive unpredictable stressors by stochastically sporulating (37, 38) or to prepare for fluctuations in the type of resources available (29–31). We showed here that the cost of phenotypic heterogeneity is mitigated when phenotype-to-fitness maps are nonlinear. In this scenario, isogenic populations of microbes can afford to maintain subpopulations of individuals that are poorly adapted to the current environment because population dynamics is dominated by phenotypic minorities. This effect has been discussed before in the context of one of the tails of a phenotypic distribution (39). Importantly, we showed that these minorities can exist in both tails of a phenotypic distribution, allowing microbes to resolve a fundamental life history trade-off by evolving phenotypic heterogeneity.

Methods

Bacterial Strains and Growth Conditions. All strains used in this study are derived from *E. coli* MG1655. Information on strains isolated from the evolution experiment is listed in *SI Appendix*, Table S1. Bacteria were grown at 37 °C in media consisting of M9 Salts, 1 mM $MgSO_4$, 0.1 mM $CaCl_2$, and

Downloaded at Palestinian Territory, occupied on December 31, 2021
www.manaraa.com

0.01% Tween 20. M9 media was supplemented with the specified sugar at the indicated concentration. All media components are from Sigma-Aldrich.

Batch Experiments. Starved cultures were started by diluting a culture grown for ~12 h from a single colony picked from a Luria-Bertani (LB) agar plate in M9 media with 1.11 mM glucose. The dilution factor used was 250-fold, and bacteria were grown in a shaking incubator at 220 rpm. After 40 h from inoculation, starved cultures were inoculated in fresh media supplemented with 1.11 mM of the indicated carbon source in 96-well plates. This corresponds to ~32 h of starvation since bacteria take ~8 h to reach the stationary phase given the dilution factor. Population growth was followed using a Synergy Microplate Spectrometer with readings taken every 3 min at 600 nm (OD_{600}). Data were smoothed using a moving average with a window of 1 h, and the maximum growth rate was calculated by using a sliding window of 9 min and finding the maximum slope of a linear least-squares fit to the log-transformed data. Only data with $OD_{600} > 0.005$ were considered due to the low reliability of the machine at lower cell densities. The derived growth parameters are unaffected by ignoring lower OD_{600} data since the instantaneous derivatives of the growth curves display a distinct single peak. Population lag time was calculated as the intersection between the regression line at the point of maximum growth rate and the $y = \log(N_0)$ line, where N_0 is the inoculation density.

Microfluidic Experiments. The mold for the microfluidic device was fabricated using standard soft lithography techniques at the FIRST clean room facility at ETH Zurich. The design consists of eight parallel channels, each of them bifurcating into two main flow channels with a height of 21 μm and a width of 200 μm. Growth channels are perpendicular to the main flow channels and have a height of 0.93 μm, a length of 25 μm, and a width ranging from 1.2 to 1.6 μm. To prepare the microfluidic device, polydimethylsiloxane (PDMS, Sylgard 184 Silicone Elastomer Kit, Dow Corning) was mixed thoroughly with a curing agent in a 10:1 ratio, poured onto the wafer, degassed using a desiccator, and cured at 80 °C for 1 h. The PDMS device was then cut out and separated from the wafer, and holes were punched for inlets and outlets. Finally, the device was bound to a microscope cover glass slide using plasma treatment.

To load cells, an overnight culture in M9 media with 5.55 mM glucose was diluted into fresh media by a 20-fold factor. Two hours later, the growing culture was concentrated by centrifugation, and cells were loaded into the microfluidic device using a pipette. Bacteria were then connected to M9 media with 1.11 mM glucose for a few hours to acclimate.

In order to starve bacteria, the microfluidic device was then connected to a bacterial culture growing from exponential to stationary phase in a 250 mL serum flask. Medium was pumped from the flask using a peristaltic pump (ISMATEC IPC-N24) with Pharmed ISMAPRENE tubing (VWR) at a rate of 0.5 mL h^{-1}. First, the flask containing only M9 media with 1.11 mM glucose was connected to the microfluidic device, and cells were loaded as described before. Then, 6 to 10 h later the flask was inoculated by diluting a culture grown for ~12 h from a single colony picked from a LB plate in M9 media with 1.11 mM glucose. The dilution factor used was 250-fold. Bacterial cultures were kept inside the microscope incubator (Life Imaging Services) at 37 °C and were constantly shaken at 320 rpm. Each channel was fed with an independent bacterial culture. After the indicated time from inoculation, the peristaltic pump was replaced by a NE-1600 syringe pump with 50 mL syringes loaded with M9 media with 1.11 mM glucose or lactose. Lag times were calculated from the time at which this switch was made. In experiments where bacteria were exposed to an antibiotic pulse, the syringes with M9 media with 1.11 mM glucose or lactose were later replaced during 80 min for syringes with the same media and 100 μg mL^{-1} of ampicillin (Sigma-Aldrich).

For experiments where bacteria underwent a diauxic shift without starvation, loading was done as indicated before, and cells remained in M9 media with 1.11 mM glucose for at least 12 h after loading. Then, we switched cells to M9 media with 1.11 mM lactose by exchanging the syringe pump. Lag time was calculated as $t_a - t_b$, where t_a is the time between the first division after the switch and the last division before the switch and t_b is the last inter-division time before the switch was made (i.e., when bacteria were still growing in glucose). We included in the analysis only cells that had divided at least three times in the 5 h preceding the switch to make sure that cells were in exponential phase when switched to lactose.

Microscopy. Microscopy was performed using a fully automated Olympus IX81 inverted microscope. Imaging was done with a 100×, numerical aperture 1.3 oil phase objective (Olympus) and an ORCA-flash 4.0 v2 sCMOS camera (Hamamatsu). Phase contrast images were taken every 12 min. Time-lapse movies were analyzed in Vanellus (40) by recording division and lysis events through visual inspection. All of the analyses presented in the paper result from quantifying the behavior of the cells at the bottom of the growth channels of the device (Fig. 1*B*). If there were two cells at the bottom of a growth channel, one was chosen at random to be analyzed. For the switches from starvation to fresh media presented in Fig. 2, a small fraction of the cells lyse without ever resuming division (less than 3% in all cases). These cells are excluded from the data to plot the lag time distributions.

Evolution Experiment. We evolved six replicate populations for reduced lag time in lactose when resuming growth after starvation. Half of the populations had as an ancestor *E. coli* MG1655 Ara+, which is the strain we use throughout the paper, and the other half had as an ancestor *E. coli* MG1655 Ara−, providing a method to check for potential cross contamination between replicate lines. All populations were started from a single colony from a LB agar plate. Bacteria were grown in 15 mL culture tubes in a shaken incubator at 37 °C and 220 rpm. Growth media had the same components as described before except for Tween 20. Glucose and lactose were added at a concentration of 0.56 mM. All populations were serially propagated for 40 cycles. In each cycle, they were first transferred to M9 media with glucose for 40 h and then to M9 media with lactose for 8 h. Cultures had a volume of 5 mL and were diluted by a 250 factor every transfer. In the final transfer every population was plated in a M9 agar plate with 0.56 mM glucose, and one colony was selected at random from the plate. This colony was grown overnight in M9 media with 0.56 mM glucose and subsequently frozen with 80% glycerol at −80 °C. The resulting colony stocks from the different populations were used to generate the data presented in Fig. 3 and *SI Appendix*, Figs. S5 and S6 and Table S1.

Sequencing and Mutation Identification. Genomic DNA of both ancestral strains and the six isolated clones was extracted using the Wizard Genomic DNA Purification Kit (Promega). Quality control and library preparation were performed by GATC (Konstanz, Germany) and sequenced on an Illumina HiSeq4000 machine using 150-base pair paired-end reads. Raw reads were trimmed, and adapters were removed using the default settings of Trimmomatic version 0.35 (41). All properly paired reads with a minimum length of 2×80 bp were kept. Sequences were aligned to the reference genome of *E. coli* MG1655 (RefSeq accession number NC_000913.2), and mutations were identified using the default settings of the breseq pipeline (version 0.30.1) (42). Mutations in each of the evolved clones were identified using gdtools by comparing to the respective sequenced ancestor.

Data Availability. Sequencing reads are publicly available on the European Nucleotide Archive (ENA) database under accession number PRJEB38320. The code for the simulations is available at DataverseNL (https://hdl.handle.net/10411/TBLEFB). Microscopy data are available upon request from the corresponding author.

ACKNOWLEDGMENTS. We thank Niklaus Zemp from the Genetic Diversity Center at ETH Zurich for support with the bioinformatic analysis and Katherine Moreno, Sophie Azevedo, and Alex von Wyl for support with the image analysis. We thank Alex Hall for kindly providing the MG1655 Ara− strain that we used as the ancestor of half of the populations from the evolution experiment. S.M.-G. and G.S.v.D. were supported by Starting Independent Researcher Grant 309555 of the European Research Council and a Vidi fellowship (864.11.012) of the Netherlands Organization for Scientific Research. D.J.K. was supported by ETH Zurich through an ETH Fellowship. S.S. was supported by SystemsX through Transition Postdoc Fellowship TPdF 2014/231. D.J.K. and M.A. were supported by Grant 31003A_149267 from the Swiss National Science Foundation. S.S. and M.A. were supported by Grant 31003A_169978 from the Swiss National Science Foundation. C.V. was supported by CASCADE Fellowship PCOFUND-GA-2012-600181. S.M.-G., D.J.K., C.V., S.S., K.S., and M.A. were supported by Eawag and ETH Zurich.

1. M. Bergkessel, D. W. Basta, D. K. Newman, The physiology of growth arrest: Uniting molecular and environmental microbiology. *Nat. Rev. Microbiol.* **14**, 549–562 (2016).
2. R. Kolter, D. A. Siegele, A. Tormo, The stationary phase of the bacterial life cycle. *Annu. Rev. Microbiol.* **47**, 855–874 (1993).
3. J. E. Hobbie, E. A. Hobbie, Microbes in nature are limited by carbon and energy: The starving-survival lifestyle in soil and consequences for estimating microbial rates. *Front. Microbiol.* **4**, 324 (2013).
4. N. Q. Balaban, J. Merrin, R. Chait, L. Kowalik, S. Leibler, Bacterial persistence as a phenotypic switch. *Science* **305**, 1622–1625 (2004).
5. C. Vulin, N. Leimer, M. Huemer, M. Ackermann, A. S. Zinkernagel, Prolonged bacterial lag time results in small colony variants that represent a sub-population of persisters. *Nat. Commun.* **9**, 4074 (2018).
6. O. Gefen, C. Gabay, M. Mumcuoglu, G. Engel, N. Q. Balaban, Single-cell protein induction dynamics reveals a period of vulnerability to antibiotics in persister bacteria. *Proc. Natl. Acad. Sci. U.S.A.* **105**, 6145–6149 (2008).

Downloaded at Palestinian Territory, occupied on December 31, 2021
www.manaraa.com

7. O. Gefen, O. Fridman, I. Ronin, N. Q. Balaban, Direct observation of single stationary-phase bacteria reveals a surprisingly long period of constant protein production activity. *Proc. Natl. Acad. Sci. U.S.A.* **111**, 556–561 (2014).
8. A. Brauner, O. Fridman, O. Gefen, N. Q. Balaban, Distinguishing between resistance, tolerance and persistence to antibiotic treatment. *Nat. Rev. Microbiol.* **14**, 320–330 (2016).
9. N. Q. Balaban *et al*., Definitions and guidelines for research on antibiotic persistence. *Nat. Rev. Microbiol.* **17**, 441–448 (2019).
10. E. Kussell, R. Kishony, N. Q. Balaban, S. Leibler, Bacterial persistence: A model of survival in changing environments. *Genetics* **169**, 1807–1814 (2005).
11. B. R. Levin, K. I. Udekwu, Population dynamics of antibiotic treatment: A mathematical model and hypotheses for time-kill and continuous-culture experiments. *Antimicrob. Agents Chemother.* **54**, 3414–3426 (2010).
12. O. Fridman, A. Goldberg, I. Ronin, N. Shoresh, N. Q. Balaban, Optimization of lag time underlies antibiotic tolerance in evolved bacterial populations. *Nature* **513**, 418–421 (2014).
13. D. Madar *et al*., Promoter activity dynamics in the lag phase of *Escherichia coli*. *BMC Syst. Biol.* **7**, 136 (2013).
14. P. J. Choi, L. Cai, K. Frieda, X. S. Xie, A stochastic single-molecule event triggers phenotype switching of a bacterial cell. *Science* **322**, 442–446 (2008).
15. J. Abramson, S. Iwata, H. R. Kaback, Lactose permease as a paradigm for membrane transport proteins (Review). *Mol. Membr. Biol.* **21**, 227–236 (2004).
16. M. J. Brauer *et al*., Conservation of the metabolomic response to starvation across two divergent microbes. *Proc. Natl. Acad. Sci. U.S.A.* **103**, 19302–19307 (2006).
17. F. Vasi, M. Travisano, R. E. Lenski, Long-term experimental evolution in *Escherichia coli*. II. Changes in life-history traits during adaptation to a seasonal environment. *Am. Nat.* **144**, 432–456 (1994).
18. S. Moreno-Gámez *et al*, Wide lag time distributions break a trade-off between reproduction and survival in bacteria. European Nucleotide Archive. https://www.ebi.ac.uk/ena/browser/view/PRJEB38320. Deposited 14 May 2020.
19. R. Figueira *et al*., Adaptation to sustained nitrogen starvation by *Escherichia coli* requires the eukaryote-like serine/threonine kinase YeaG. *Sci. Rep.* **5**, 17524 (2015).
20. T. M. Conrad *et al*., Whole-genome resequencing of *Escherichia coli* K-12 MG1655 undergoing short-term laboratory evolution in lactate minimal media reveals flexible selection of adaptive mutations. *Genome Biol.* **10**, R118 (2009).
21. J. L. W. V. Jensen, Sur les fonctions convexes et les inégalités entre les valeurs moyennes. *Acta Math.* **30**, 175–193 (1906).
22. J. Baranyi, Stochastic modelling of bacterial lag phase. *Int. J. Food Microbiol.* **73**, 203–206 (2002).
23. Z. Kutalik, M. Razaz, J. Baranyi, Connection between stochastic and deterministic modelling of microbial growth. *J. Theor. Biol.* **232**, 285–299 (2005).
24. C. A. Fux, J. W. Costerton, P. S. Stewart, P. Stoodley, Survival strategies of infectious biofilms. *Trends Microbiol.* **13**, 34–40 (2005).
25. A. L. Koch, The adaptive responses of *Escherichia coli* to a feast and famine existence. *Adv. Microb. Physiol.* **6**, 147–217 (1971).
26. B. Beckert *et al*., Structure of a hibernating 100S ribosome reveals an inactive conformation of the ribosomal protein S1. *Nat. Microbiol.* **3**, 1115–1121 (2018).
27. D. W. Gohara, M. F. Yap, Survival of the drowsiest: The hibernating 100S ribosome in bacterial stress management. *Curr. Genet.* **64**, 753–760 (2018).
28. F. K. Vasi, R. E. Lenski, Ecological strategies and fitness tradeoffs in *Escherichia coli* mutants adapted to prolonged starvation. *J. Genet.* **78**, 43–49 (1999).
29. A. Solopova *et al*., Bet-hedging during bacterial diauxic shift. *Proc. Natl. Acad. Sci. U.S.A.* **111**, 7427–7432 (2014).
30. O. Kotte, B. Volkmer, J. L. Radzikowski, M. Heinemann, Phenotypic bistability in *Escherichia coli*'s central carbon metabolism. *Mol. Syst. Biol.* **10**, 736 (2014).
31. A. M. New *et al*., Different levels of catabolite repression optimize growth in stable and variable environments. *PLoS Biol.* **12**, e1001764 (2014).
32. N. Geisel, J. M. G. Vilar, J. M. Rubi, Optimal resting-growth strategies of microbial populations in fluctuating environments. *PLoS One* **6**, e18622 (2011).
33. W. C. Ratcliff, R. F. Denison, Individual-level bet hedging in the bacterium *Sinorhizobium meliloti*. *Curr. Biol.* **20**, 1740–1744 (2010).
34. O. S. Venturelli, I. Zuleta, R. M. Murray, H. El-Samad, Population diversification in a yeast metabolic program promotes anticipation of environmental shifts. *PLoS Biol.* **13**, e1002042 (2015).
35. E. S. Wright, K. H. Vetsigian, Stochastic exits from dormancy give rise to heavy-tailed distributions of descendants in bacterial populations. *Mol. Ecol.* **28**, 3915–3928 (2019).
36. B. Eldon, J. Wakeley, Coalescent processes when the distribution of offspring number among individuals is highly skewed. *Genetics* **172**, 2621–2633 (2006).
37. J.-W. Veening *et al*., Bet-hedging and epigenetic inheritance in bacterial cell development. *Proc. Natl. Acad. Sci. U.S.A.* **105**, 4393–4398 (2008).
38. M. Fujita, R. Losick, Evidence that entry into sporulation in *Bacillus subtilis* is governed by a gradual increase in the level and activity of the master regulator Spo0A. *Genes Dev.* **19**, 2236–2244 (2005).
39. A. J. Waite *et al*., Non-genetic diversity modulates population performance. *Mol. Syst. Biol.* **12**, 895 (2016).
40. D. J. Kiviet, Vanellus (2019). Available at: https://github.com/daankiviet/vanellus. Accessed 11 February 2019.
41. A. M. Bolger, M. Lohse, B. Usadel, Trimmomatic: A flexible trimmer for Illumina sequence data. *Bioinformatics* **30**, 2114–2120 (2014).
42. D. E. Deatherage, J. E. Barrick, Identification of mutations in laboratory-evolved microbes from next-generation sequencing data using breseq. *Methods Mol. Biol.* **1151**, 165–188 (2014).

Downloaded at Palestinian Territory, occupied on December 31, 2021

www.manaraa.com